UKAEA FUS 445

EURATOM/UKAEA Fusion

The role of polarization current in magnetic island evolution

J W Connor, F L Waelbroeck* and H R Wilson

January 2001

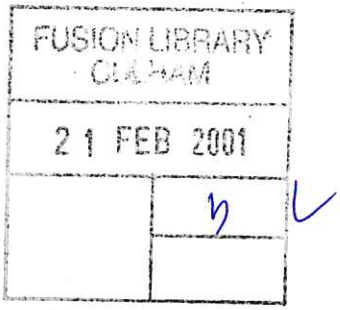

(This report also appears at
http://w3fusion.ph.utexas.edu/ifs/reports2000.html
as Institute of Fusion Studies report IFSR#897)

EURATOM/UKAEA Fusion Association

Culham Science Centre, Abingdon
Oxfordshire, OX14 3DB
United Kingdom
Telephone +44 1235 464131
Facsimile +44 1235 463435

The role of polarization current in magnetic island evolution

J. W. Connor*, F. L. Waelbroeck†, and H. R. Wilson*

January 17, 2001

Abstract

The polarization current plays an important role in the evolution of magnetic islands with a width comparable to the characteristic ion orbit width. Understanding the evolution of such small magnetic islands is important for two reasons: (1) to investigate the threshold mechanisms for growth of large-scale islands (e.g. neoclassical tearing modes), and (2) to describe the drive mechanisms for small scale magnetic turbulence and consequent transport. This paper presents a two-fluid, cold ion, collisional analysis of the role of the polarization current in magnetic island evolution in slab geometry. It focuses on the role played by the conjunction of parallel electron dynamics and perpendicular transport (particle diffusion and viscosity) in determining the island rotation frequency and the distribution of the polarization current within the island.

1 Introduction

The role of the polarization current in the non-linear evolution of thin islands was first investigated by Garbet *et al.* [1, 2] and Rebut and Hugon[3] using kinetic theory, and by Smolyakov[4] using fluid theory. A very complete bibliography of early work is given in Smolyakov's review of nonlinear island

*EURATOM/UKAEA Fusion, Culham Science Centre, Abingdon, Oxfordshire, OX14 3DB, United Kingdom

†Institute for Fusion Studies, University of Texas, Austin, Texas 78712, USA

evolution in inhomogeneous plasmas. [5] It has since been studied extensively both in slab[6, 7] and toroidal [8, 9, 10] geometry.

The majority of the literature considers a regime such that the ratio ρ_*/w of the Larmor radius to the island width is small and develops expansions in powers of this ratio. [4, 5, 6, 7, 8, 9, 10] Here ρ_* is the larger of the ion Larmor radius ρ_i and the sonic Larmor radius $\rho_s = c_s/|\omega_{ci}|$, where $c_s = \sqrt{T_e/m_i}$ is the speed of sound and ω_{ci} is the ion gyrofrequency. The results can be expressed in terms of the quantity $\Delta_{\rm pol}$ that parameterizes the effect of the polarization current on stability:

$$\Delta_{\rm pol} = 4\,g\,\frac{L_s^2}{w^3}\,\frac{\omega(\omega-\omega_{*i})}{k^2 v_A^2}, \tag{1}$$

where $\Delta_{\rm pol} < 0$ indicates that the polarization current is stabilizing. Here ω and ω_{*i} are the island rotation and ion diamagnetic frequencies, L_s is the magnetic shear length, k is the wavenumber along the island chain, $v_A = B_0/\sqrt{4\pi n m_i}$ is the Alfvén velocity, and g is a geometric coefficient. The effect of the polarization current clearly depends on the sign of the coefficient g. The value of g, and particularly its sign, is the subject of the present paper.

The value of g depends on the velocity profile across the island. The authors investigating the $w \gg \rho_*$ limit[4, 5, 6, 7, 8, 9, 10] considered velocity profiles that were discontinuous across the separatrix and approximately constant in magnitude outside the separatrix, modeling an island slicing through the plasma much like a sailing vessel through the seas. They found that $g < 0$, and concluded that the polarization current is destabilizing when the island is rotating at a frequency lying in the range between the ion drift frequency and the guiding-center drift frequency of the unperturbed plasma. They further concluded that the polarization current would be stabilizing for frequencies lying outside this range. These conclusions led to models for anomalous transport [4, 6, 7] and to a possible explanation of the observed threshold island size for neoclassical magnetic islands. [9, 10] The latter are presently the subject of wide concern as a result of the threat they pose to the performance of Next Step tokamaks.

The conclusions of References 4-10 regarding the limit $w \gg \rho_*$ are in conflict, however, with the conclusions reached in References 3 and 11-12. In Reference 3, Rebut and Hugon carried out a kinetic calculation, taking into account the finite Larmor radius of the ions in order to study the effect of the polarization current on an island close to the stochastic threshold. They

found that the polarization current was destabilizing for islands rotating in the electron diamagnetic direction, in conflict with References 4-10. The discrepancy between the results of Rebut and Hugon[3] and References 4-10 can be understood in light of the results of References 11-12, which studied the effect of the polarization current on the interaction of magnetic islands with external structures. Fitzpatrick *et al.*[12], in particular, examined a family of continuous velocity profiles. The results show that as a velocity profile develops a pedestal at the island separatrix, a substantial fraction of the polarization current becomes concentrated in the layer where the velocity is changing rapidly. The contribution of this layer was omitted in References 4-10, resulting in an underestimate for g.

In many applications of interest, however, the width of the layer where the velocity changes rapidly is comparable to the ion-sound Larmor radius ρ_s. In such narrow layers, collisional effects and nonlinearities that are neglected by Rebut and Hugon[3] are important. Equally important are the drifts and electron parallel dynamics effects that are omitted from the magnetohydrodynamic (MHD) model used in References 11-12. A recent investigation [13] has addressed the question of the role of the layer using a model in which the electron temperature is treated as small, and the problem is solved analytically by expanding in powers of $k_r\rho_i$, keeping higher order terms to improve the treatment of the separatrix layer (where $k_r\rho_i \sim 1$ in general). Here, we present a solution of the drift-MHD equations with cold ions that includes the effects of the nonlinearity of the ion response as well as the effects of collisions[14]. We find that the layer width scales as ρ_s in this low ion temperature limit, so that we can consistently neglect finite ion Larmor radius effects, $k_r\rho_i \ll 1$, as well as ion diamagnetic drift effects.

The paper is set out as follows. We begin by describing in Section 2 the sheared slab magnetic geometry and the equation governing island evolution. We then introduce in Section 3 the fluid model that forms the basis for our calculations. As previously mentioned this model assumes that $T_i \ll T_e$, where T_i and T_e are respectively the ion and electron temperatures. In Section 4 we present the equilibrium solutions of this model. These are magnetic islands rotating at approximately constant frequency and evolving at a rate determined by transport processes. We present, in particular, an explicit solution for a model such that the electrons respond non-linearly to the magnetic perturbations, but the ion motion is dominated by a linear response to the electrostatic perturbations. In this model the width of the separa-

trix layer is of order $\rho_s/\sqrt{1-\omega_{*e}/\omega}$, where $\omega_{*e} = -k\rho_s c_s/L_n$ is the electron diamagnetic frequency. Here $L_n = n/(dn/dX)$, where X is the coordinate transverse to the magnetic surfaces. In order to overcome the assumption of a linear ion response, we develop in Section 5 a theory of transport near magnetic islands. The results of this theory take the form of a set of one-dimensional transport equations that govern the evolution of the profiles across the island. After presenting the analytic solutions of these transport equations in relevant limits, we describe their numerical solution. The precise form of the electrostatic non-linearities in the resulting ion response determines the layer width, and this leads to a slight modification of the role of the polarization current. In Section 6 we draw conclusions, and discuss the consequences for tearing mode evolution in tokamaks.

2 Magnetic Geometry and Ampère's Law

We consider a periodic sheared slab geometry with a magnetic field given by

$$\mathbf{B} = B_0\hat{\mathbf{z}} - \nabla\psi(X,\xi)\times\hat{\mathbf{z}}, \tag{2}$$

where B_0 is a constant magnetic field pointing in the symmetry direction $\hat{\mathbf{z}} = \nabla Z$, and where the azimuthal magnetic flux ψ is related to the longitudinal vector potential A_Z by $\psi = -A_Z$. The reference state is chosen such that $\psi_0 = -B_0X^2/2L_s$, where L_s is the magnetic shear length. We consider a perturbed azimuthal flux of the form $\psi = \psi_0 + \tilde{\psi}\cos\xi$, where ξ is the azimuthal angle (note, X, ξ and Z form an orthogonal coordinate system). This perturbed flux describes a magnetic island of half-width w given by

$$w = \sqrt{\frac{4L_s\tilde{\psi}}{B_0}}. \tag{3}$$

We will use the normalized flux-surface label χ defined by

$$\chi^2 = \frac{\tilde{\psi}-\psi}{2\tilde{\psi}} = x^2 + \sin^2\frac{\xi}{2}, \tag{4}$$

where $x = X/w$. We have defined χ so that $\chi = 0$ is the island 'O'-point, $\chi = 1$ is the island separatrix and $\chi > 1$ is the region outside the island. At large distances from the island, $\chi \sim |x|$. It is often convenient to use χ as the transverse variable, rather than x.

The above sheared-slab geometry can be considered to model a large aspect-ratio tokamak by making the correspondence $x = (r - r_s)/w$, where r is the minor radius and $r = r_s$ is the radius of the resonant surface, and $\xi = m\theta - n\zeta - \int^t \omega(t')dt'$ where θ and ζ are the poloidal and toroidal angles, m and n are the poloidal and toroidal mode numbers, and ω is the propagation frequency of the island, which in general depends on the time t. The shear-length is related to the tokamak parameters by $L_s = Rq/s$, where R is the major radius, q is the safety factor, and $s = (r/q)dq/dr$ is the magnetic shear.

We will assume that the constant-$\tilde{\psi}$ approximation holds: $\tilde{\psi} \gg \partial_x \tilde{\psi}$. Following Rutherford,[15] we integrate Ampère's law radially across the island region (i.e. where $J_\parallel$ is localized). Taking the $\cos\xi$ component of both sides, and matching this to the linear solution away from the island, we arrive at the equation determining the island evolution:

$$\oint d\xi \int_{-\infty}^{\infty} dx\, J_\parallel \cos\xi = \frac{c\Delta'}{4w}\tilde{\psi}, \tag{5}$$

where

$$\Delta' = \frac{1}{\tilde{\psi}}\left(\left.\frac{\partial\tilde{\psi}}{\partial X}\right|_{X=0^+} - \left.\frac{\partial\tilde{\psi}}{\partial X}\right|_{X=0^-}\right) \tag{6}$$

and $0^\pm$ indicates the asymptotic limits as X approaches the resonant surface from either side.

From the asymptotic matching, Eq. (5), and Ohm's law, it follows that we can write the island evolution equation in the form:

$$\frac{dw}{dt} \propto \Delta' + \Delta_{\rm pol}, \tag{7}$$

where Δ' represents the free energy available in the equilibrium current density profile, and $\Delta_{\rm pol}$ is the contribution to the free energy from the polarization current:

$$\Delta_{\rm pol} = -\frac{16L_s}{cB_0 w}\oint d\xi \int_{-\infty}^{\infty} dx\, J_{\rm pol}\cos\xi, \tag{8}$$

where $J_{\rm pol}$ represents the polarization current.

Our aim is to calculate $J_{\rm pol}$, and use Eq (8) to evaluate its effects on the island evolution.

3 Fluid Model

In order to investigate the basic properties of small scale magnetic islands, we adopt a two-fluid, cold ion model ($T_i = 0$) based on the Braginskii equations [14]. We denote the convective time derivative along the $\mathbf{E} \times \mathbf{B}$ flow by D/Dt,

$$\frac{D}{Dt} = \frac{\partial}{\partial t} + \mathbf{v}_E \cdot \boldsymbol{\nabla},$$

where $\mathbf{v}_E$, the electric drift velocity, is related to the electrostatic potential ϕ by $\mathbf{v}_E = (c/B_0)\hat{\mathbf{z}} \times \boldsymbol{\nabla}\phi$. Note that since $T_i = 0$, $\mathbf{v}_E$ is approximately equal to the ion fluid velocity.

We are interested in narrow islands, $k_{\|} c_s \ll \omega_*$, where $k_{\|}$ is the parallel component of the wavevector and c_s is the sound speed. For such islands we may neglect the ion parallel motion. The electron continuity equation is then

$$\frac{Dn}{Dt} = \frac{1}{e}\nabla_{\|} J_{\|} + D\boldsymbol{\nabla}_{\perp}^2 n, \tag{9}$$

where n is the density (equal for ions and electrons by quasi-neutrality), e is the electron charge, $\nabla_{\|} = (\mathbf{B}/B) \cdot \boldsymbol{\nabla}$ and $\boldsymbol{\nabla}_{\perp}$ represent the gradients, respectively, along and transverse to the magnetic field, and D is the radial (ambipolar) diffusion coefficient. For the case of classical transport,

$$D = \beta_e \frac{c^2}{8\pi\sigma_{\|}},$$

where $\beta_e = 8\pi n T_e/B^2$, T_e is the electron temperature, and $\sigma_{\|}$ is the parallel electrical conductivity.

The quasi-neutrality condition requires $\nabla \cdot \mathbf{J} = 0$, or

$$\nabla_{\|} J_{\|} = \frac{c^2}{4\pi v_A^2}\left[\frac{DU}{Dt} - \mu\boldsymbol{\nabla}_{\perp}^2 U\right], \tag{10}$$

where $U = \boldsymbol{\nabla}_{\perp}^2\phi$ is proportional to the vorticity, and μ is the viscosity. Eq. (10) can be viewed alternatively as a vorticity or a local torque-balance equation.

For Ohm's law we use

$$E_{\|} + \frac{\nabla_{\|} p}{ne} = \frac{J_{\|}}{\sigma_{\|}} - \alpha\frac{\nabla_{\|} T_e}{e}, \tag{11}$$

where $E_\parallel = (1/c)\partial\psi/\partial t - \nabla_\parallel\phi$ is the parallel electric field, p is the plasma pressure, and $\alpha = 0.71$ is the coefficient describing the effect of the thermal force.

Lastly we describe the electron temperature evolution [5] with the equation

$$\frac{3}{2}n\frac{DT_e}{Dt} = \nabla_\parallel(\kappa_\parallel\nabla_\parallel T_e) + \kappa_\perp\nabla_\perp^2 T_e + (1+\alpha)\nabla_\parallel\left(\frac{J_\parallel T_e}{e}\right), \qquad (12)$$

where $\kappa_{\parallel,\perp}$ are the parallel and perpendicular thermal heat conductivities, respectively.

Equations (9)-(12) describe a collection of processes that occur on several disparate time-scales. These may be grouped into fast and slow processes. The fast processes consist of parallel temperature equilibration and of dynamical evolution under the effect of force imbalance, such as drift-Alfvén motion. The slow processes, by contrast, consist of perpendicular transport. Two comments are appropriate here. First, the ability to distinguish the dynamical from the perpendicular transport time-scales is a defining property of nonlinear island theory (in linear theory, the layer widths are determined by the balance between transport and dynamical processes). Second, states that are stationary or in equilibrium on the fast time scale include states with steady–state island rotation. In fact, such rotation is a salient feature of all the solutions obtained here.

The separation of time scales described above forms the basis for reducing the two-dimensional system of equations (9)-(12) to a one-dimensional system of *transport* equations describing the evolution of the profiles of particle density, temperature, electric potential, and current-density across the island. Our approach is closely analogous to that used to derive neoclassical transport equations in the Pfirsch-Schlüter regime. We proceed in two steps. First, we seek an equilibrium solution ($\partial/\partial t = 0$) neglecting the perpendicular transport terms. We find that the equilibrium solution depends on a family of undetermined profile functions. Second, we obtain equations for the profile functions from the solvability conditions for the equations that determine the corrections to the equilibrium resulting from the perpendicular transport terms.

In the following section, we present equilibrium solutions for the fluid model described in Eqs. (9)-(12), and briefly discuss the solution of these equations for model profiles. We then describe the derivation of the transport equations and their numerical solution in Section 5.

4 Drift-Alfvén Equilibrium

4.1 Generalized Grad-Shafranov equations

The equilibrium equations are obtained by neglecting the perpendicular transport terms in Eqs. (9)-(11), and setting all the time derivatives equal to zero. Note that the latter step implicitly fixes the frame of observation to be that moving with the island. The equilibrium equations are

$$\mathbf{v}_E \cdot \boldsymbol{\nabla} n = \frac{1}{e}\nabla_{\|} J_{\|}; \tag{13}$$

$$\nabla_{\|} J_{\|} = \frac{c^2}{4\pi v_A^2}\, \mathbf{v}_E \cdot \boldsymbol{\nabla} U; \tag{14}$$

$$\frac{1}{n}\nabla_{\|} n - \frac{e\nabla_{\|}\phi}{T_e} = -(1+\alpha)\frac{\nabla_{\|} T_e}{T_e}. \tag{15}$$

The heat equation, Eq. (12), is structurally different from the others in that the parallel transport term dominates the dynamic terms. Stationarity thus requires

$$\nabla_{\|}(\kappa_{\|}\nabla_{\|} T_e) = 0. \tag{16}$$

The solution of the heat equation is simply

$$T_e = T_\sigma(\chi), \tag{17}$$

where $\sigma = \pm$ distinguishes the temperature profile to the right $(+)$ and left $(-)$ of the island (inside the island, $T_+(\chi) = T_-(\chi) = T(\chi)$).

Using the solution of the heat equation to simplify Ohm's law and integrating the remaining terms yields the Maxwell-Boltzmann law

$$n = N_\sigma(\chi)\exp\left(\frac{e\phi}{T_e}\right), \tag{18}$$

where $N_\sigma(\chi)$ is an integration constant. We adopt the convention that $\phi(x = 0, \xi = 0) = 0$. Since the variation of the density across the island is of order $w/r_s \ll 1$, it is convenient to introduce the normalized perturbed density $\tilde{n} = (n - n_0)/n_0'$, where $n_0 = N(0)$ is the density at the O-point of the island and $n_0' = (dn/dx)_{x \gg w}$. We also introduce the normalized potential $\varphi = -kc\phi/Bw\omega_{*e} = (e\phi/T_e)(L_n/w)$. Keeping only terms of first-order in the island width, the Maxwell-Boltzmann relation takes the form

$$\tilde{n} = \varphi + H_\sigma(\chi), \tag{19}$$

where $H_\sigma(\chi) = (N_\sigma(\chi) - n_0)/n_0'$ is proportional to the profile-function h of Wilson *et al.* [9].

To solve the remaining two equations, (13)-(14), we eliminate the magnetic derivative of $J_\parallel$ and integrate the resulting equation along the equipotentials, or ion streamlines. We find

$$\rho_s^2 \nabla_\perp^2 \varphi - \tilde{n} = L_\lambda(\varphi), \tag{20}$$

where $L_\lambda(\varphi)$ is an undetermined integration constant. We have included the subscript λ in order to allow for the possibility that L takes different values on distinct equipotentials corresponding to the same value of φ. We note that the quantity on the left hand side of Eq. (20) is conserved in the absence of dissipation, as seen by eliminating the current from Eqs. (9) and (10). An analogous quantity, called the potential vorticity, plays an important role in geophysical fluid dynamics.

We may eliminate the density from Eqs. (19)-(20) in order to obtain an equation for φ in terms of the profile functions. We find

$$\rho_s^2 \nabla_\perp^2 \varphi - K_\lambda(\varphi) = H_\sigma(\chi), \tag{21}$$

where $K_\lambda(\varphi) = L_\lambda(\varphi) + \varphi$. This equation plays a role analogous to that of the Grad-Shafranov equation in tokamak equilibria: it determines the geometry of the equipotentials, or ion streamlines, in terms of the two profile functions H and K. The profile functions themselves must be determined from the transport analysis.

In order to completely specify the potential, it is necessary to supply boundary conditions to Eq. (21). From Taylor-series expansion of the unperturbed density, we see that the density perturbation must be odd to lowest order in the island width. Likewise, the odd part of the electrostatic potential dominates (in fact, the contribution of the even part of φ to Δ_{pol} vanishes identically in a viscously relaxed state [11]). We thus restrict consideration to states such that the density and electrostatic potential are odd with respect to the resonant surface. For such states, $H_\sigma(\chi) = \sigma H(\chi)$ and thus $H(\chi) = 0$ for $\chi < 1$ (i.e. inside the separatrix). Likewise, $T_\sigma(\chi) = \sigma T(\chi)$. Consistent with our choice of parity, we will further assume that $K_\lambda(\varphi) = K(\varphi)$ is one-to-one (the solutions we calculate for φ are invertible).

The assumption of odd parity yields the first boundary condition on φ, $\varphi(x = 0, \xi) = 0$. The second boundary condition consists of matching the asymptotic electric field at large distances from the island to the electric field

in the reference state. Note that the asymptotic electric drift velocity in the island's rest frame is the negative of the island phase velocity in the frame where the electric field vanishes. Thus, our second boundary condition is $\partial\varphi/\partial x \to \omega/\omega_{*e}$, where ω is the island rotation frequency in the frame where the electric field vanishes far from the island.

We complete the solution of the equilibrium problem by integrating the continuity equation, Eq. (13), along the magnetic field line after eliminating the density with the help of Eq. (19). In doing this we use the fact that

$$\mathbf{v}_E \cdot \nabla\psi = -c\nabla_\parallel\phi. \tag{22}$$

We find

$$J_\parallel = \frac{n_0 ec}{4\tilde{\psi}\chi}\frac{dH}{d\chi}\sigma\phi + I(\chi), \tag{23}$$

where $I(\chi)$ is an integration constant. The average along the field lines of $J_\parallel$ (and thus $I(\chi)$), is determined by Ohm's law: this is the inductive current. The oscillatory part of $J_\parallel$, obtained by subtracting from $J_\parallel$ its average value, is the polarization current:

$$\frac{J_{\rm pol}}{n_0 ec_s} = \frac{\rho_s}{w}\frac{L_s}{L_n}\frac{\sigma}{\chi}\frac{dH}{d\chi}\left(\varphi - \frac{\langle\varphi\rangle_\chi}{\langle 1\rangle_\chi}\right). \tag{24}$$

Here we have introduced the flux-surface average,

$$\langle f\rangle_\chi = \begin{cases} \oint \dfrac{d\xi}{2\pi}\dfrac{f}{|\partial_x\chi|}, & \chi > 1; \\ \displaystyle\sum_\sigma \oint \frac{d\xi}{2\pi}\frac{\Theta(\chi - |\sin(\xi/2)|)f}{|\partial_x\chi|}, & \chi \le 1, \end{cases} \tag{25}$$

where Θ is the Heaviside step-function. Note that in a torus, the oscillatory part also contains a contribution from the Pfirsch-Schlüter current that gives rise to a stabilizing effect, as shown by Kotschenreuther *et al.*[16]

Substituting the polarization current into the equation for $\Delta_{\rm pol}$, we obtain the $T_i = 0$ limit of Eq. (1), with

$$g = -\left(\frac{\omega_{*e}w}{\omega\rho_s}\right)^2 \oint\frac{d\xi}{\pi}\int_{-\infty}^{\infty} dx\,\frac{\sigma}{\chi}\frac{dH}{d\chi}\left(\varphi - \frac{\langle\varphi\rangle_\chi}{\langle 1\rangle_\chi}\right)\cos\xi.$$

An equivalent form for g that is often more convenient is

$$g = -\left(\frac{\omega_{*e}w}{\omega\rho_s}\right)^2 \oint\frac{d\xi}{\pi}\int_{-\infty}^{\infty} \frac{dx}{\chi}\frac{dH}{d\chi}\,\sigma\varphi\left(\cos\xi - \frac{\langle\cos\xi\rangle_\chi}{\langle 1\rangle_\chi}\right). \tag{26}$$

Our task is thus to solve Eq. (21) for φ, and to substitute the result in Eq. (26) in order to calculate g. Note that φ is clearly a function of ρ_s/w through Eq. (21). Less visibly, it also depends on the island rotation frequency ω/ω_{*e} through the boundary conditions.

4.2 MHD limit

We begin by showing how the MHD results can be recovered from the two-fluid equilibrium equations obtained above in the limit where $\rho_s \to 0$. We seek an asymptotic solution in the form

$$\varphi = \varphi_0 + (\rho_s/w)\varphi_1 + (\rho_s/w)^2\varphi_2 + \cdots \tag{27}$$

Substituting the above expansion in Eq. (21), we find that to lowest order

$$\varphi_0 = \sigma\Phi(\chi) \equiv K^{-1}[-\sigma H(\chi)], \tag{28}$$

where K^{-1} is the inverse of the function K. Note that Φ, like H, vanishes identically inside the island. Equation (28) shows that, to lowest order, the plasma flow is confined within the flux surfaces. Substituting the solution in Eq. (28) into the term proportional to ρ_s^2 in Eq. (21) yields the next-order correction,

$$\varphi_2 = \frac{\sigma}{K'[\Phi(\chi)]}\frac{\partial^2\Phi}{\partial x^2}. \tag{29}$$

We use the convention that a prime denotes differentiation with respect to a function's argument (here $K' = dK/d\Phi$). Using the lowest order solution (28), we see that the denominator in Eq. (29) is

$$K'[\Phi(\chi)] = -\frac{H'(\chi)}{\Phi'(\chi)}.$$

Substituting our solution for φ into the definition of g, we now recover the MHD result

$$g_{\mathrm{MHD}} = \int_0^\infty \frac{d\chi}{\chi}\frac{d}{d\chi}\left(\frac{1}{\chi}\frac{d\hat{\Phi}}{d\chi}\right)^2\left(\langle\cos^2\xi\rangle_\chi - \frac{\langle\cos\xi\rangle_\chi^2}{\langle 1\rangle_\chi}\right), \tag{30}$$

where

$$\hat{\Phi} = \frac{\omega_{*e}}{\omega}\Phi$$

is the electric potential normalized so that $\partial\hat{\Phi}/\partial x \to 1$ far from the island.

The difficulty with velocity profiles that are discontinuous on the separatrix is immediately apparent from Eq. (30). For such profiles, the integrand of g contains a contribution from a delta-function multiplying some very rapidly varying geometrical coefficients. Evaluating Eq. (30) with this delta-function, we find

$$g_{\mathrm{MHD}} = g_\delta + g_{\mathrm{ext}}, \tag{31}$$

where

$$g_\delta = \frac{16}{3\pi}\left(\hat{\Phi}'(1^+)\right)^2 \tag{32}$$

is the contribution from the delta-function and

$$g_{\mathrm{ext}} = \int_{1+}^{\infty} \frac{d\chi}{\chi}\frac{d}{d\chi}\left(\frac{1}{\chi}\frac{d\hat{\Phi}}{d\chi}\right)^2\left(\langle\cos^2\xi\rangle_\chi - \frac{\langle\cos\xi\rangle_\chi^2}{\langle 1\rangle_\chi}\right) \tag{33}$$

is the contribution from the velocity outside the separatrix. It is natural to ask, however, whether g_{MHD} gives an accurate representation of the effect of the polarization current, especially in the presence of drifts and related effects. We consider this question next.

4.3 Small ρ_s/w corrections to MHD

In order to resolve the question of the accuracy of the MHD approximation, we return to the asymptotic solution [Eq. (27)] and note that if Φ has a discontinuous derivative, the small-ρ_s ordering breaks down in a layer of width ρ_s around the discontinuity. In this layer $(\rho_s/w)^2\partial^2\varphi/\partial x^2$, φ, H, K, and ρ_s/w are all comparable. Assuming that K and H are well behaved at the separatrix, we may use in the layer an alternative expansion based on the "distance" to the separatrix. To lowest order, Eq. (21) becomes

$$\rho^2\nabla_\perp^2\varphi - \varphi = -\varphi_{\mathrm{ext}}, \tag{34}$$

where

$$\rho = \frac{\rho_s}{\sqrt{K'(0)}}$$

describes the layer width and

$$\varphi_{\mathrm{ext}}(x,\xi) = a\,\sigma\left(|x| - \cos(\xi/2)\right)\Theta\left(|x| - \cos(\xi/2)\right) \tag{35}$$

is simply the first term in the series expansion of the external solution, Eq. (28), about the separatrix. Here

$$a = \Phi'(1)\cos(\xi/2).$$

Note that if $K(\varphi)$ is linear, $K'(0) = 1 - \omega_{*e}/\omega$. For $K'(0) < 0$ (or if $K(\varphi)$ is linear, for $0 < \omega < \omega_{*e}$) the equation for the potential admits oscillatory solutions: that is, the island excites drift waves. We will not consider this case here, except for a brief discussion in Sec. 4.5

The solution of the layer equation, Eq. (34), is

$$\varphi(x,\xi) = \varphi_{\rm ext}(x,\xi) + (\rho/w)\varphi_1(x,\xi), \tag{36}$$

where

$$\varphi_1(x,\xi) = \frac{\sigma a}{2}\left(e^{-||x|-|\cos(\xi/2)||/\rho} - e^{-(|x|+|\cos(\xi/2)|)/\rho}\right) \tag{37}$$

is proportional to the Green's function for the differential operator on the left of Eq. (34). The discontinuity in the derivative of φ_1 cancels that in $\varphi_{\rm ext}$. Our solution, Eq. (36), thus shows that parallel electron streaming resolves the discontinuity in the electric drift velocity in a layer of width ρ. Note that the second term in φ_1 is only important close to the X-point where $\cos(\xi/2) \sim \rho$.

Since φ_1 decays exponentially outside the layer, the asymptotic expansion Eq. (27) with φ_0, φ_1, and φ_2 given by Eqs. (28), (29) and (37) is in fact uniformly valid inside as well as outside the layer. We may thus calculate g by substituting Eq. (27) in the definition of g. We find that $g = g_{\rm ext} + g_{\rm ped}$, where $g_{\rm ext}$ is the contribution to g from flows outside the velocity pedestal given in Eq. (33) and

$$g_{\rm ped} = \left(\frac{\omega_{*e}w}{\omega\rho_s}\right)^2 \oint \frac{d\xi}{\pi}\int_{-\infty}^{\infty} dx\, \frac{dH}{d\chi}\frac{\rho\sigma\varphi_1}{w\chi}\left(\cos\xi - \frac{\langle\cos\xi\rangle_\chi}{\langle 1\rangle_\chi}\right). \tag{38}$$

is the contribution from the velocity pedestal in the separatrix layer. We may estimate the latter contribution by expanding the geometric coefficients in the vicinity of the separatrix. We find

$$g_{\rm ped} = g_\delta\left(1 - 3\left[\ln(8w/\rho)\right]^{-1}\right), \tag{39}$$

where g_δ is the contribution of the delta-function in Eq. (30). Equation (39) shows that the correction to the MHD result arising from small but finite ρ/w is substantial, and it even suggests that g changes sign near $\rho/w = 0.1$. This is not the case, however, as we will see from the numerical and large ρ_s solution.

4.4 Large ρ_s/w solution

We next consider the solution of Eq. (21) for large ρ_s/w. Here, the vorticity term dominates so that to lowest order

$$\nabla_\perp^2 \varphi_0 = 0.$$

The solution is simply

$$\varphi_0 = \frac{\omega}{\omega_{*e}}\, x. \tag{40}$$

Substituting this in Eq. (26), we find

$$g = \mathcal{I}\,\frac{w^2}{\rho^2} = \mathcal{I}\,\frac{w^2}{\rho_s^2}\left(1 - \frac{\omega_{*e}}{\omega}\right). \tag{41}$$

Here

$$\mathcal{I} = -4\int_1^\infty d\chi \frac{d\hat{H}}{d\chi}\frac{\langle \cos\xi\rangle_\chi}{\langle 1\rangle_\chi} > 0,$$

where $\hat{H}(\chi) = H(\chi)/[(1-\omega/\omega_{*e})]$. Equation (41) is in agreement with the results of previous authors.[19, 4, 7] The polarization drift is thus destabilizing for frequencies outside the electron drift band $\{0, \omega_{*e}\}$. Inside the electron drift band, the excitation of electron drift waves (discussed in the next section) prevents us from drawing firm conclusions but the above result suggests that the polarization drift is likely to be stabilizing.

4.5 Numerical solution for linear ion response

We now present the results of numerical solutions of Eq. (21) showing how the polarization current affects the island evolution for finite values of ρ_s/w. These results complement the small and large ρ_s/w asymptotic formulae obtained above. We use a model in which $K(\varphi)$ is taken to be linear. This model is equivalent to assuming that the flattening of the electron density and temperature across the island constitutes the dominant non-linearity, and that the ion response to the electrostatic perturbations associated with the island is approximately linear.

For linear $K(\varphi)$, the solution of Eq. (21) depends only on $\rho = \rho_s/(1-\omega_{*e}/\omega)^{1/2}$. We begin by commenting on the case when $\rho^2 < 0$, which occurs when $0 < \omega < \omega_{*e}$ (i.e. when the island propagates in the electron drift direction, but more slowly than the electron diamagnetic frequency in the

frame where the radial electric field far from the island is zero). In this case the solutions are oscillatory in the radial coordinate, and the effect of the separatrix layer extends far beyond the separatrix region. The physical interpretation is as follows. In the vicinity of the island separatrix, a wide range of wavelengths are driven by the delta-function contained in H''. As a result, the island resonates with an electron drift wave whenever the mode frequency satisfies $0 < \omega < \omega_{*e}$. This electron drift wave propagates away from the island towards the regions of strong ion Landau damping. The excitation of waves in numerical simulations of linear drift-tearing modes has been reported previously by Biskamp.[17]

The fluid model used here fails to capture the full physics of this effect because of the assumption that $k_{\|} v_{th,i} \ll \omega$. The electron drift wave carries energy out from the island to large distances where $\omega \simeq k_{\|} v_{th,i}$, where it is dissipated by ion Landau damping (here $k_{\|} = kx/L_s$ is the parallel wave number and $v_{th,i}$ is the ion thermal velocity). The effect of such islands is therefore not simply localized on the w length-scale, but extends instead to distances $\sim \sqrt{T_e/T_i}(L_s/L_n)\rho_s\omega/\omega_{*e} \gg w$. Of course, new dissipative processes associated with the ion Landau damping will likely have an impact on the solution for ω as well as on $\Delta'_{\rm pol}$. While the physics of such modes is certainly interesting and warrants further exploration in the future, we restrict our attention here to the more localized modes having $\rho^2 > 0$.

We have considered three distinct forms for the profile $H(\chi) = (1 - \omega/\omega_{*e})\hat{H}(\chi)$. In the limit where the profile relaxes to a steady-state governed by transport, the form of $H(\chi)$ is given by Eq. (64) of Sec. 5.4. We have also considered two alternative models. The first of these is similar to the profile introduced by Smolyakov,[5] modified so as to make $\hat{H}$ continuous:

$$\hat{H}(\chi) = \hat{H}_S(\chi) \equiv (\sqrt{\chi^2 - 1/2} - \sqrt{1/2})\,\Theta(\chi - 1). \tag{42}$$

This profile is very similar to the relaxed profile, Eq. (64): their derivatives are compared in Fig. 1. The last model we have considered is

$$\hat{H}(\chi) = (\chi - 1)\,\Theta(\chi - 1), \tag{43}$$

representing a simple, linear dependence on χ outside the separatrix. Table 1 lists the numerical values of the various constants for these three profiles.

For numerical simplicity, we have used the Smolyakov profile Eq. (42) in the numerical integration of Eq. (21). In Fig. 2 we take $\rho/w = 0.2$ and plot the solution for φ as a function of x across the island 'O'-point ($\xi = 0$) and

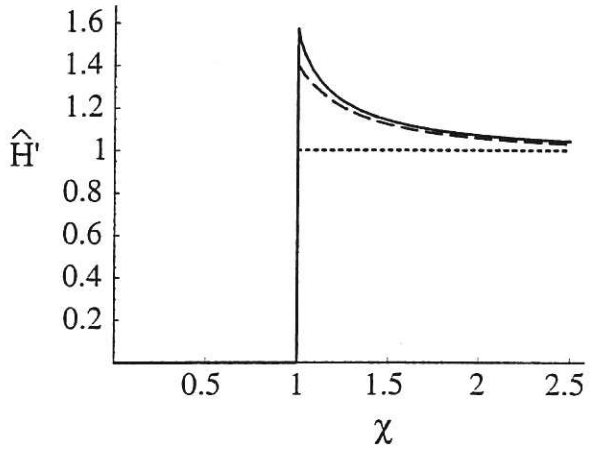

Figure 1: Stability coefficient g, defined in Eqs. (1) and (26), as a function of $\rho/w = (\rho_s/w)(1-\omega_{*e}/\omega)^{-1/2}$ for linear $K(\varphi)$.

across the island 'X'-point ($\xi = \pi$); the dashed curves show the the small ρ/w expansion of the exterior solution given in Eqs. (28)-(29). Note how the discontinuity in φ at the island separatrix (i.e. $x = 1$ in Fig. 2a) is smoothed by the finite ρ/w effects, while further from the island the $x - \cos\xi/2 \gg \rho$ expansion and numerical solution are in agreement. The complete asymptotic solution, shown as the dotted lines in Fig. 2, is in good agreement with the numerical solution even close to the separatrix.

In Fig. 3 we show the results for g and compare them to the asymptotic results in the limit of small and large ρ/w. The comparison shows that the asymptotic formula is only accurate at extremely small ρ/w. The error originates in the asymptotic evaluation of the g integral, and is due to the poor convergence properties of the expansion in powers of $[\log(\rho/w)]^{-1}$ used

Table 1: Numerical parameters for the various models of the $H(\chi)$ profile

Model	Eq.	g_δ	g_{ext}	g_{MHD}	$\mathcal{I}$
Smolyakov	(42)	$32/3\pi \cong 3.40$	-1.06	2.34	0.39
transport	(64)	$4\pi/3 \cong 4.19$	-1.43	2.76	0.40
linear-χ	(43)	$16/3\pi \cong 1.70$	-0.44	1.26	0.34

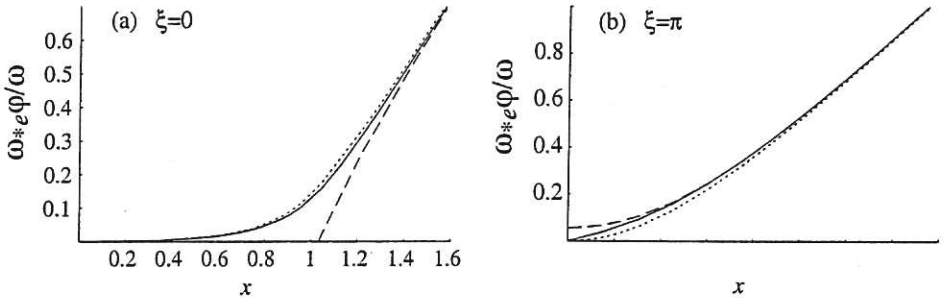

Figure 2: Comparison of the forms of $d\hat{H}/d\chi$ corresponding to the transport solution, Eq. (64) (full curve), the simplified expressions of Eq. (42) (dashed curve), and Eq. (43) (dotted line).

to describe the geometric coefficients near the separatrix.

In conclusion, we see that MHD substantially overestimates the destabilizing effect of the velocity pedestal but correctly predicts the sign of g. That is, the polarization current is destabilizing, but its magnitude is much reduced compared to the MHD prediction.

5 Transport

The transport of particles, momentum and heat across a magnetic island is a complex problem that remains incompletely understood. A particular source of difficulty is the breakdown of the transport ordering: the separation between the time-scale for ideal (drift or MHD) motion and the time-scale for non-ideal (collisional) processes. For large islands the breakdown of the transport ordering occurs either in narrow layers surrounding the separatrix or near the X-point. One manifestation of this breakdown is the incomplete flattening of the temperature in very thin islands due to the competition between parallel and perpendicular transport near the separatrix,[18] or between parallel transport and convective drifts. [19]

In order to lay the foundations for future work on island transport, we begin by deriving transport equations that are *independent* of the transport ordering. We next apply the transport ordering and the equilibrium results of Sec. 4 in order to obtain equations that specify the unknown profile functions T, H, and K that appear in the solution of the equilibrium equations.

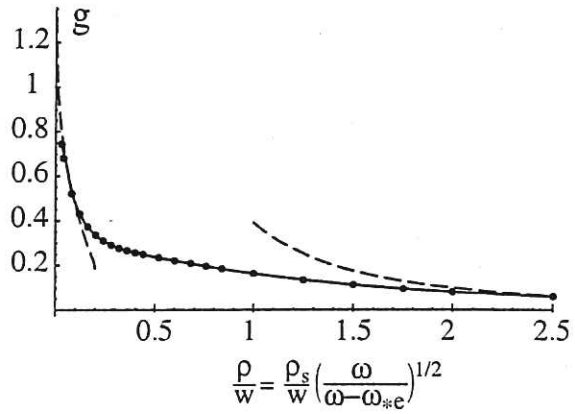

Figure 3: Electrostatic potential φ for $\rho/w = 0.2$ on a chord crossing the island O-point (a) and X-point (b) for a linear $K(\varphi)$. The full curve shows the numerical solution of Eq. (21) and the dashed curve shows the asymptotic solution away from the separatrix ($\chi - 1 \gg \rho_s/w$) given in Eqs. (28)-(29). The dotted line shows the complete asymptotic solution for small ρ/w given in Eqs. (36)-(37).

Lastly, we complete the section by presenting numerical solutions of the profile equations.

5.1 General transport laws

We derive here a set of transport equations from the steady-state limit ($\partial/\partial t = 0$) of the fluid equations (9)-(12). The transport equations consist simply of the solubility conditions for the fluid equations.

The first transport equation is simply the flux-surface average of Ohm's law,

$$\frac{1}{c}\left\langle \frac{\partial \psi}{\partial t} \right\rangle_\chi = \frac{1}{\sigma_\parallel} \left\langle J_\parallel \right\rangle_\chi . \tag{44}$$

In the steady-state limit, $\partial\tilde{\psi}/\partial t = 0$ and the average current in the island is equal to the inductive current in the reference (unperturbed) state.

The second transport equation is only slightly more complicated. It follows from the ion continuity equation, which is obtained by eliminating the

current between Eqs. (9) and (10),

$$\frac{Dn}{Dt} - \frac{c^2}{4\pi e v_A^2}\left[\frac{DU}{Dt} - \mu\nabla_\perp^2 U\right] = D\nabla_\perp^2 n. \tag{45}$$

Setting the time derivatives to zero, we see that the resulting equation consists of transport terms and convective derivatives due to the electric drift velocity. Since the physical variables are single-valued, the integral of the convective derivatives along a closed streamline must vanish. This motivates us to introduce an average along streamlines, $\langle\cdot\rangle_\varphi$, that plays a similar role to the flux-surface average $\langle\cdot\rangle_\chi$ introduced in Eq. (25). Assuming that φ is a single-valued function of ξ, we define

$$\langle f\rangle_\varphi = \oint \frac{d\xi}{2\pi}\frac{f}{\varphi_x}, \tag{46}$$

where the integral is to be carried out along an equipotential. The subscript x denotes partial differentiation: $\varphi_x \equiv \partial\varphi/\partial x$. Generalization to more complicated streamline topology is straightforward but unnecessary for our purposes.

Applying the streamline average to the ion continuity equation yields the second transport equation,

$$\mu\rho_s^2\left\langle\nabla_\perp^4\varphi\right\rangle_\varphi = D\left\langle\nabla_\perp^2\tilde{n}\right\rangle_\varphi. \tag{47}$$

We may integrate this equation once by using Gauss's law,

$$\langle\nabla\cdot\Gamma\rangle_\varphi = \frac{d}{d\varphi}\langle\Gamma\cdot\nabla\varphi\rangle_\varphi.$$

There follows

$$D\langle\partial^\varphi\tilde{n}\rangle_\varphi - \mu\rho_s^2\langle\partial^\varphi\nabla_\perp^2\varphi\rangle_\varphi = D/w^2, \tag{48}$$

where we have used the asymptotic boundary condition $n \sim n_0(1 + X/L_n)$. Here $\partial^\varphi f = \nabla f\cdot\nabla\varphi$ is the contravariant φ-component of the gradient of f. Equation (48) expresses the conservation of ions: the first term on the left-hand side is the ambipolar flux caused by the drift associated with the electron-ion friction forces, and the second term represents the non-ambipolar flux resulting from the drift associated with the viscous forces. The sum of these terms equals the particle flux in the reference state given in the right-hand side.

The third transport equation expresses the conservation of electrons. We obtain it by taking the flux-surface average of the electron continuity equation,

$$\langle \mathbf{v}_E \cdot \nabla n \rangle_\chi = D \left\langle \nabla_\perp^2 n \right\rangle_\chi . \tag{49}$$

The term on the left-hand side of this equation vanishes when evaluated with the lowest-order solution, Eq. (19), confirming that it is in fact a transport term. We may integrate Eq. (49) by observing that by virtue of the incompressibility of the electric drift, the electric convective derivative is the divergence of the convection flux,

$$\mathbf{v}_E \cdot \nabla n = \nabla \cdot (n \mathbf{v}_E). \tag{50}$$

We integrate this equation once by using Gauss's law in the form,

$$\langle \nabla \cdot \Gamma \rangle_\chi = \frac{d}{d\chi} \langle \Gamma \cdot \nabla \chi \rangle_\chi .$$

We find

$$D \langle \partial^\chi n \rangle_\chi - \langle n v_E^\chi \rangle_\chi = D n_0 / w L_n, \tag{51}$$

where we have again used the asymptotic boundary conditions. Here $\partial^\chi n = \nabla n \cdot \nabla \chi$ and $v_E^\chi = \mathbf{v}_E \cdot \nabla \chi$. Equation (51) expresses conservation of electron flux: the first term on the left-hand side is the ambipolar diffusion flux, and the second term is the convective flux caused by the electric drift across flux surfaces. The sum of these terms equals the particle flux in the reference state given in the right-hand side. Note that the flux caused by the electric drift did not appear in the ion equation, Eq. (48), because that equation describes the fluxes across stream-surfaces. A disagreeable feature of Eq. (51) is that although the electric-drift term is a transport flux, as noted above, it possesses no simple expression in terms of a sum of transport coefficients multiplying thermodynamic forces. We will show below a partial remedy based on combining the electron and heat conservation equations.

The fourth transport equation, expressing the conservation of heat, is formally identical to Eq. (51). We obtain it by taking the flux-surface average of the heat equation,

$$n_0 \langle \mathbf{v}_E \cdot \nabla T_e \rangle_\chi = \kappa_\perp \left\langle \nabla_\perp^2 T_e \right\rangle_\chi . \tag{52}$$

Performing the same manipulations as for the particle flux, we arrive at

$$\kappa_\perp \langle \partial^\chi T_e \rangle_\chi - n_0 \langle T_e v_E^\chi \rangle_\chi = \kappa_\perp T_e / w L_T. \tag{53}$$

Equation (53) expresses conservation of the heat flux. The terms in this equation have analogous interpretations to those in the particle transport equation.

We next show how to eliminate the electric-drift fluxes in Eqs. (51) and (53) in favor of explicit transport fluxes. To this end, note that Eq. (22) allows us to express the electric-drift fluxes in terms of the gradient of the convected quantities along the magnetic field,

$$\langle f v_E^\chi \rangle_\chi = \frac{\rho_s c_s L_s}{w L_n \chi} \left\langle f \nabla_\parallel \varphi \right\rangle_\chi = -\frac{\rho_s c_s L_s}{w L_n \chi} \langle \varphi \nabla_\parallel f \rangle_\chi, \tag{54}$$

where f stands for n or T_e. The purpose of this substitution is to make use of Ohm's law,

$$\langle \varphi \nabla_\parallel n \rangle_\chi = \frac{n_0 e}{T_e \sigma_\parallel} \langle \varphi J_\parallel \rangle_\chi - (1+\alpha) \frac{n_0}{T_e} \langle \varphi \nabla_\parallel T_e \rangle_\chi, \tag{55}$$

to evaluate the electric drift fluxes. Equation (55) expresses the fact that the electric-drift component of the particle flux is produced by the combination of electron-ion drag, pressure, and thermoelectric forces along the magnetic field. We now obtain an equation consisting entirely of explicit transport terms by combining Eqs. (51) and (53)-(55),

$$D \left(\langle \partial^\chi n \rangle_\chi - \frac{n_0}{w L_n} \right) + \kappa_\perp (1+\alpha) \left(\frac{\langle \partial^\chi T_e \rangle_\chi}{T_e} - \frac{1}{w L_T} \right) = -\frac{L_s}{w L_n \chi} \frac{n_0 c}{B_0 \sigma_\parallel} \langle \varphi J_\parallel \rangle_\chi. \tag{56}$$

This may be used to replace either the electron or heat conservation equations in the final set of transport equations.

We next apply the transport ordering and replace the fields in the transport laws by their equilibrium values. This yields equations for the profile functions.

5.2 Profile equations under the transport ordering

We consider here islands of sufficient width as to satisfy the transport ordering:

$$\nu_\perp \ll \omega_{*e} \ll \frac{\kappa_\parallel}{n} \nabla_\parallel^2,$$

where $\nu_\perp \sim \kappa_\perp / (n w^2)$ represents the rate of perpendicular transport. This allows us to substitute the equilibrium results obtained in Sec 4.1 into the

steady-state transport laws derived above, and obtain a set of equations determining the profile functions H, T, and K

We begin by substituting the equilibrium solutions Eqs. (19) and (21) into Eq. (48). This yields an equation for $K(\varphi)$ in terms of $H(\chi)$ and φ,

$$K'(\varphi) = \frac{D}{\mu}\left(1 - \frac{1}{\langle\varphi_x^2\rangle_\varphi}\right) + \sigma\left(\frac{D}{\mu} - 1\right)\frac{\langle\varphi_x\partial_x H(\chi)\rangle_\varphi}{\langle\varphi_x^2\rangle_\varphi}. \tag{57}$$

We may obtain an equation for $H(\chi)$ by solving the electron continuity and heat equations. Before doing this, however, we must find the variation of the temperature along the magnetic field lines in order to express the convective heat transport in Eq. (53) explicitly as a transport term.

To find the variation of the temperature along the magnetic field lines, we solve the heat equation (12) for the parallel gradient of the temperature. Keeping only terms of order $\omega_{*e}T_e$, we have

$$\nabla_\parallel(\kappa_\parallel\nabla_\parallel T_e) = \frac{3}{2}n\mathbf{v}_E\cdot\boldsymbol{\nabla}T_e - (1+\alpha)\nabla_\parallel\left(\frac{T_e J_\parallel}{e}\right). \tag{58}$$

Using the result that $T_e = \sigma T(\chi)$ to leading order, as found in Eq. (17), Eq. (58) is easily integrated:

$$\kappa_\parallel\nabla_\parallel T_e = \frac{3}{2}n_0\sigma T'\frac{\rho_s c_s L_s}{wL_n\chi}\left(\varphi - \frac{\langle\varphi\rangle_\chi}{\langle 1\rangle_\chi}\right) - (1+\alpha)\sigma T\frac{J_{\rm pol}}{e}. \tag{59}$$

Substituting the parallel temperature gradient into the heat conservation equation (53), using Eqs(24) and (54), and solving for T'/T yields

$$\frac{T'}{T} = \frac{(1+\alpha)\iota\Upsilon H' + \eta_e}{\frac{3}{2}\iota\Upsilon + 2E/\pi}\frac{w}{L_n}, \tag{60}$$

where $\eta_e = L_n/L_T$, $E = E(\chi^{-2})$ is the complete elliptic integral of the second kind, ι is a constant given by

$$\iota = \frac{(\rho_s c_s n_0)^2}{\kappa_\parallel\kappa_\perp}\frac{L_s^2}{L_n^2}$$

and Υ is the function of χ defined by

$$\Upsilon = \frac{1}{\chi^2}\left(\langle\varphi^2\rangle_\chi - \frac{\langle\varphi\rangle_\chi^2}{\langle 1\rangle_\chi}\right).$$

Lastly, we solve for H' by using Eq. (60) to eliminate the temperature from Eq. (56). We find

$$H' = \frac{\delta\left(1 - \frac{\sigma}{\chi}\langle x\partial_x\varphi\rangle_\chi\right)\left(2E/\pi + \frac{3}{2}\iota\Upsilon\right) + (1+\alpha)\frac{3}{2}\eta_e\iota\Upsilon}{(2\delta E/\pi + \gamma\Upsilon)\left(2E/\pi + \frac{3}{2}\iota\Upsilon\right) + 2(1+\alpha)^2\iota\Upsilon E/\pi}. \qquad (61)$$

Here

$$\gamma = \frac{(\rho_s c_s n_0 e)^2}{T_e \sigma_\parallel \kappa_\perp}\frac{L_s^2}{L_n^2} \qquad \text{and} \qquad \delta = \frac{D n_0}{\kappa_\perp}.$$

Together, the set of profile equations (57), (60), and (61) determine K, T, and H in terms of φ alone. We next show that these equations have a rotating solution: that is, the island has non-zero frequency in the frame where the unperturbed electric drift vanishes. To show this we consider two important limiting cases.

5.3 Classical transport in weakly sheared field

In the case of classical transport the coefficients appearing in H' take the values

$$\gamma = 0.11\frac{L_s^2}{L_n^2}; \qquad \iota = 0.068\frac{L_s^2}{L_n^2}; \qquad \delta = 1.$$

We consider the limit of weak shear, $L_n/L_s \ll 1$, pertinent for stellarators and large aspect-ratio tokamaks. In this limit, $H' \sim (L_n/L_s)^2 \ll 1$. A solution that satisfies both the electrostatic Grad-Shafranov equation, Eq. (21), and the ion flux-conservation equation, Eq. (57), is

$$\varphi = \tilde{n} + O(L_n/L_s)^2 = x + O(L_n/L_s)^2.$$

The above solution describes an island rotating at approximately the electron diamagnetic frequency, $\omega \simeq \omega_{*e} + O(L_n^2/L_s^2)$. At this frequency the island is co-rotating with the electron fluid. The ions, by contrast, drift through the island under the effect of the electric field. This makes it possible for the density gradient to maintain itself in the island. Since the ions are unaccelerated, however, the polarization current is small in the weak shear classical limit, as can be seen from Eq. (24). For this reason we will not describe this solution further here.

5.4 Case of strong perpendicular heat transport

A more realistic ordering than the classical transport ordering discussed above is to assume that the perpendicular heat conductivity is strongly anomalous. Specifically, we assume that $\iota \sim \gamma \ll 1$, but that the perpendicular heat diffusivity nevertheless satisfies the transport ordering:

$$\frac{\rho_s c_s n_0}{\kappa_\parallel} \sim \frac{\rho_s c_s n_0 e^2}{T_e \sigma_\parallel} \ll \frac{L_n^2}{L_s^2} \frac{\kappa_\perp}{\rho_s c_s n_0} \ll k L_n \frac{w^2}{L_s^2},$$

where the last inequality expresses the transport ordering.

With the above assumptions, the solubility condition for the heat conduction equation reduces to

$$\kappa_\perp \left\langle \nabla_\perp^2 T(\chi) \right\rangle_\chi = 0. \tag{62}$$

The solution is

$$\frac{T'}{T} = \frac{w}{L_T} \frac{\pi \Theta(\chi - 1)}{2E(\chi^{-2})}. \tag{63}$$

The above temperature profile is identical to that found by Rutherford [15].

We next consider the expression for H'. In order to decouple the calculation of H from that of φ, we assume that particle diffusion is at most moderately anomalous, in the sense that $\delta \ll \iota \sim \gamma$ or

$$\frac{D}{\rho_s c_s} \frac{L_n^2}{L_s^2} \ll \frac{\rho_s n_0 c_s}{\kappa_\parallel} \sim \frac{\rho_s c_s n_0 e^2}{T_e \sigma_\parallel}.$$

When the above condition is satisfied, Eq. (61) shows that $H(\chi)$ is independent of φ. There follows

$$H' = \frac{L_n}{w} \frac{T'}{T \eta_c} = \frac{\eta}{\eta_c} \frac{\pi \Theta(\chi - 1)}{2E(\chi^{-2})}, \tag{64}$$

where

$$\eta_c = \frac{2}{3} \left(1 + \alpha + \frac{e^2 \kappa_\parallel}{T \sigma_\parallel (1 + \alpha)} \right). \tag{65}$$

For classical parallel transport coefficients, $\eta_c = 1.75$.

The asymptotic behavior of H, $H \sim (1 - \omega/\omega_{*e})x$, determines the island rotation frequency:

$$\omega = \left(1 - \frac{\eta_e}{\eta_c} \right) \omega_{*e}. \tag{66}$$

The above solution for ω is the same as that obtained by Smolyakov [5] neglecting viscosity and radial diffusion, and using an energy conservation law. Strictly, we should retain the propagation frequency evolution terms to demonstrate that this is a stable solution. This would complicate the algebra considerably, but we note that the derivation of Smolyakov [5] does demonstrate that this is a stable solution. While it is possible that the separatrix layer may modify this result, we leave the study of this to future work.

It is appropriate here to make two comments on the form of $H(\chi)$: (1) its derivative is discontinuous at the island separatrix ($\chi = 1$) and (2) its second derivative is logarithmically divergent as the island separatrix is approached. The discontinuity in the derivative of $H(\chi)$ is the feature which was neglected in References 4-10, and is the basic source of the discrepancy between these references and the results of Rebut and Hugon[3]. It is therefore important to retain this feature. The logarithmic singularity, on the other hand, provides a negligible contribution to Eq. (26) and it is safely neglected. Therefore, to avoid the numerical complication associated with the form of $H(\chi)$ given in Eq. (64), we will again use the simpler form $H_S(\chi)$ given in Eq. (42).

In summary, we replace the solution for the $H(\chi)$ profile given Eq. (64) with the model profile given in Eq. (42). We are then faced with the task of solving the system consisting of Eqs. (21) and (57) for φ and K. This is a difficult task because one cannot calculate the averages over the constant φ surfaces until one knows the form for φ, and one cannot solve for φ until one knows the form of $K(\varphi)$.

5.5 Solution of the transport equation in the viscous limit

We can gain some insight into the transport properties by considering the asymptotic solution for φ away from the separatrix, $x - \cos(\xi/2) \gg \rho_s/w$, where φ is constant on the perturbed flux surfaces, i.e. $\varphi = \Phi(\chi)$. In this limit it is more convenient to use the form of the ion conservation equation given in Eq. (48). For $\varphi = \Phi(\chi)$, this equation takes the form

$$\frac{\mu\rho_s^2}{Dw^2}\frac{d}{d\chi}\left(\langle\chi_x^4\rangle_\chi\frac{dv}{d\chi}\right) - \langle\chi_x^2\rangle_\chi v = \langle\chi_x^2\rangle_\chi H' - 1, \tag{67}$$

where $v = d\varphi/d\chi$ is proportional to the flux-surface average of the velocity, $\langle \chi_x^2 \rangle_\chi = 2E(\chi^{-2})/\pi$, and

$$\langle \chi_x^4 \rangle_\chi = \frac{2}{3\pi}\left[2(2-\chi^{-2})E(\chi^{-2}) - (1-\chi^{-2})K(\chi^{-2})\right].$$

Here $K(\chi^{-2})$ is the complete elliptic integral of the first kind. Equation (67) shows that the transport processes introduce a new radial length scale into the system: $\sqrt{\mu/D}\rho_s$.

We can obtain solutions to Eq. (67) in two limits. When $\rho_s^2 \ll \mu\rho_s^2/D \ll w^2$, the first term is only important near the separatrix, where it smooths the velocity distribution. We may thus approximate the coefficients of Eq. (67) by their values on the separatrix. We require that v be continuous at the separatrix ($v(1) = 0$). The solution, after substituting the value of H' given in Eq. (64), is

$$v(\chi) = \frac{\pi}{2}\frac{\omega}{\omega_{*e}}\left\{\frac{1}{E(\chi^{-2})} - \exp\left[-\frac{w(\chi-1)}{\rho_s\lambda_s}\sqrt{\frac{D}{\mu}}\right]\right\}, \tag{68}$$

where $\lambda_s = \sqrt{2/3}$ and $\chi > 1$. Note that for consistency with the assumption $\varphi = \Phi(\chi)$ it is necessary that the viscous layer be much wider than ρ_s. This is the case when $D \ll \mu$.

The second solution corresponds to the limit where the velocity localization width greatly exceeds the island width. This occurs when $w^2 \ll \mu\rho_s^2/D$. In this case the solution is

$$v(\chi) = \frac{\omega}{\omega_{*e}}\left[1 - \exp\left(-\frac{w(\chi-1)}{\rho_s\lambda_\infty}\sqrt{\frac{D}{\mu}}\right)\right], \tag{69}$$

where $\lambda_\infty = 1$ and $\chi > 1$. Since the velocity vanishes in the proximity of the island, the polarization current is negligible in this limit. Note that for $w^2 \sim \mu\rho_s^2/D$, Eq. (68) can be used as a rough approximation by suitably adjusting λ between λ_s and λ_∞.

In the absence of particle diffusion ($D \to 0$) we see that, for the model we are using, the 'transport' length scale $\sim \sqrt{\mu/D}\rho_s$ becomes very large, so that one needs to go to very large distances from the island to recover the linear dependence of φ with x expected in the absence of the island; thus the effect of the island is not radially localized in this limit. One can see qualitatively why we should expect this to be the case by considering the following simple

model. Suppose we impose a flow $v = v_0$ associated with the dynamics of the island, and initially localized around the island. This profile will evolve under the action of viscosity; a simple model equation describing the evolution of v is

$$\frac{\partial v}{\partial t} = \frac{\mu}{w^2}\frac{\partial^2 v}{\partial \chi^2}. \tag{70}$$

This is to be solved subject to the boundary condition $v = v_0(\chi)$ at time $t = 0$. We assume that there is no flow inside the island in this example: $v = 0$ at the island separatrix, $\chi = 1$. The solution can be constructed from the appropriate Green's function, [20]

$$v = v_0 \text{ erf}\left[\frac{w(\chi - 1)}{\sqrt{4\mu t}}\right], \tag{71}$$

where erf is the error function. Clearly flows localized on the island width length scale can exist for short times, $t \ll \mu/w^2$, but Eq. (71) shows that eventually the island will be brought into co-rotation with the rest of the plasma (i.e. $v = 0$ everywhere).

In the presence of particle diffusion, by contrast, Eq. (68) predicts a localized, steady state solution for the flow. Remarkably, Eq. (68) further predicts that viscosity only affects the localization width of the flow, and not its amplitude. That is, the island rotation frequency is independent of μ. Note that for turbulence-dominated transport models, for which we expect $\mu \sim D$, the velocity pedestal outside the separatrix has a width comparable to ρ_s. For such models the asymptotic analysis presented above is inapplicable. We next present numerical results for the solution of Eqs. (21) and (57) in the regime where $\mu \sim D$.

5.6 Numerical solution of the transport equations

We present here the numerical solutions of equations (21) and (57), providing more quantitative details of the effect of the transport processes on both the radial structure of the electrostatic potential and on the polarization current.

The numerical procedure we have developed is the following. At each iteration i we have a form for K_i and a solution φ_i, where K_i is calculated from Eq. (57) using the solution φ_{i-1} to evaluate the averages at constant φ. We impose the boundary condition $K(0) = 0$, and write $K(\varphi) = K_L + \epsilon(K_{NL} - K_L)$, where $K_L(\varphi) = (1 - \omega_{*e}/\omega)\varphi$ is the linear form, and K_{NL} is

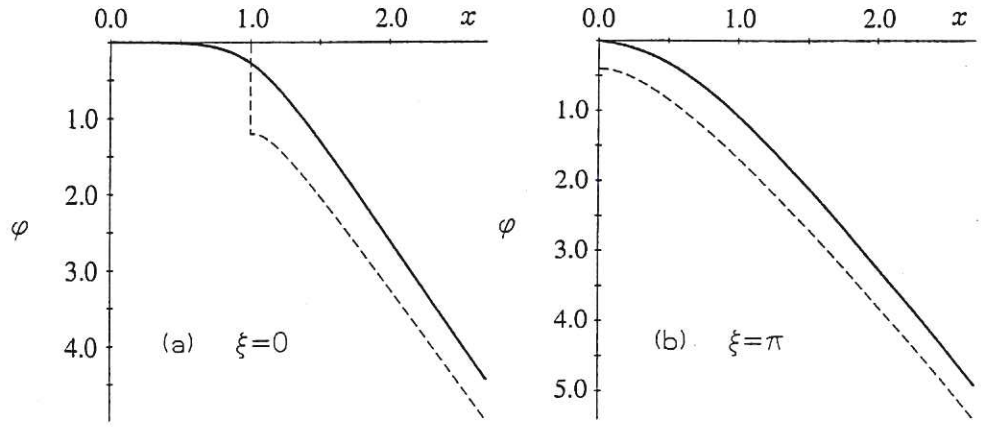

Figure 4: The full curve shows the electrostatic potential φ determined by dissipative relaxation (transport). The two profiles shown correspond to chords that cross the island's O-point (a) and X-point (b). The dashed curves are the corresponding $\chi - 1 \gg \rho_s/w$ asymptotic solution for linear $K(\varphi)$ [Eqs. (27)-(29)]. The parameters are $\rho_s/w = 0.4$, $\omega/\omega_{*e} = -2.5$ and $\mu/D = 1$.

the non-linear form derived from Eq. (57), and slowly step ϵ up from a small value $\epsilon \ll 1$ to $\epsilon = 1$ at the end of the iteration procedure. The results which we present in this section are the fully converged solutions.

We begin by considering the case $\mu = D$ (i.e. equal viscosity and diffusion). In this case the linear solution $K(\varphi) = K_L(\varphi) \to \varphi$ is an exact solution in the limit $\omega/\omega_{*e} \to \infty$. The trivial solution $K(\varphi) = 0$, corresponding to $\omega = \omega_{*e}$, constitutes a second exact solution. These two exact solutions serve as useful references for the numerical solutions. Figures 4 and 5 show the solutions for $\varphi(x, \xi = 0)$, $\varphi(x, \xi = \pi)$, and $K(\varphi)$ for the parameters $\rho_s/w = 0.4$, $\omega/\omega_{*e} = -2.5$. The solution for $\omega/\omega_{*e} \to \infty$, $K(\varphi) = \varphi$, is also shown for comparison (dash-dotted line). From Fig. 5 we see that for these parameters the dominant non-linearity in $K(\varphi)$ arises inside the island separatrix, and leads to a more pronounced flattening of φ in this region than occurs for linear K (compare Figs 2a and 4a). In Figs 6 and 7 we show the situation for islands propagating in the electron direction, $\omega/\omega_{*e} = 1.5$, $\rho_s/w = 0.4$. In this situation we see that $K(\varphi)$ becomes much flatter inside the island separatrix compared to the linear model (Fig 7); the result of this is that φ is not flat inside the island, but has a more linear dependence with x: that

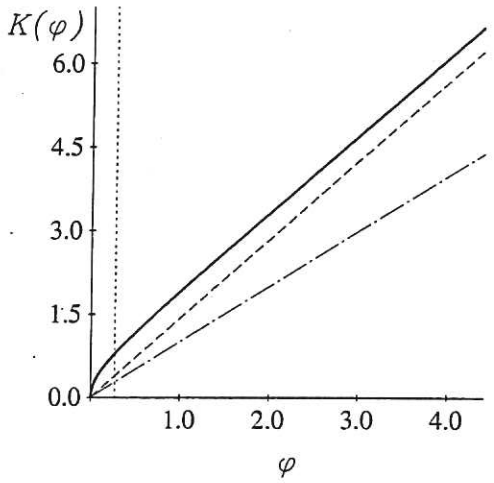

Figure 5: Relaxed non-linear $K(\varphi)$ (full curve) and linear $K(\varphi)$ (dashed curve) for the parameters of Fig 4. The vertical dotted line represents the value of φ at the island separatrix, opposite the O-point, i.e., $\varphi(x = 1, \xi = 0)$. The dash-dotted line represents the solution $K(\varphi) = \varphi$ corresponding to the limit $\omega \gg \omega_{*e}$

is, there is an electic drift through the island. Figure 8 shows how g varies with ρ^2/w^2. Comparing with Fig 3 for the linear $K(\varphi)$ model we see that the dependence of g on ρ^2/w^2 has changed significantly, although the polarization current remains destabilizing. Note that for the non-linear $K(\varphi)$ model, g depends on both ρ^2/w^2 and ρ_s/w: examples for two values of ρ_s/w are shown in Fig 8.

We have also considered cases where viscosity dominates radial diffusion. In Fig 9 we show the dependence of g on the ratio μ/D; we see that for the value of $\omega/\omega_{*e} = 1.5$, g is relatively independent of μ/D. In Fig 10 we show the radial form of φ for $\mu/D = 10$; it is more broad than the corresponding form for $\mu/D = 1$, as expected from Eq. (68). Note, however, that the assumptions underlying Eq. (68) are not satisfied by the parameters of Fig. 10. Specifically, $\rho_s/w = 0.4$ is too large for the asymptotic analysis to be successful, so that Eq. (68) only indicates the qualitative nature of the solution.

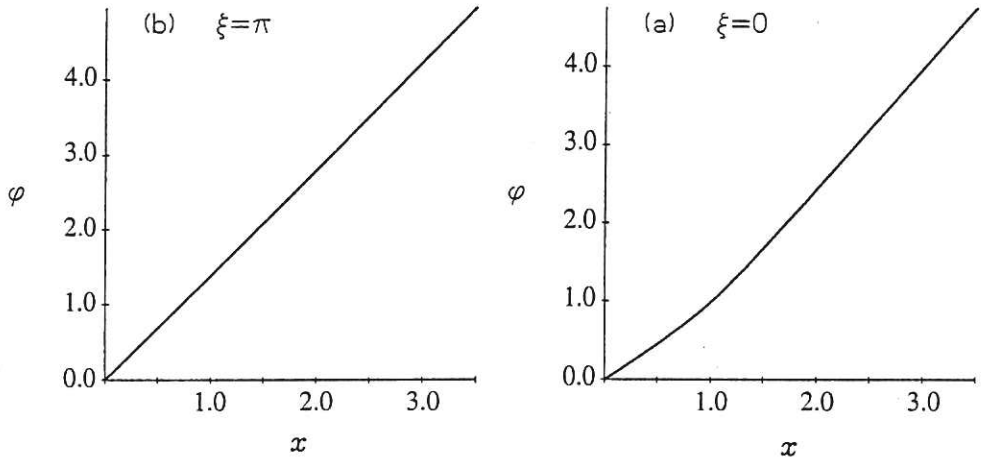

Figure 6: Electrostatic potential φ determined by dissipative relaxation (transport). The two profiles shown cross the island O-point (a) and X-point (b). The parameters are $\rho_s/w = 0.4$, $\omega/\omega_{*e} = 1.5$ and $\mu/D = 1$.

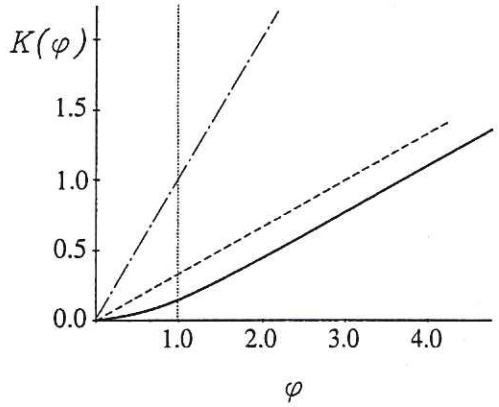

Figure 7: Relaxed non-linear $K(\varphi)$ (full curve) and linear $K(\varphi)$ (dashed curve) for the parameters of Fig 6. The vertical dotted line represents the value of φ at the island separatrix, opposite the O-point, *i.e.* $\varphi(x = 1, \xi = 0)$. The dash-dotted line represents the solution $K(\varphi) = \varphi$ corresponding to the limit $\omega \gg \omega_{*e}$

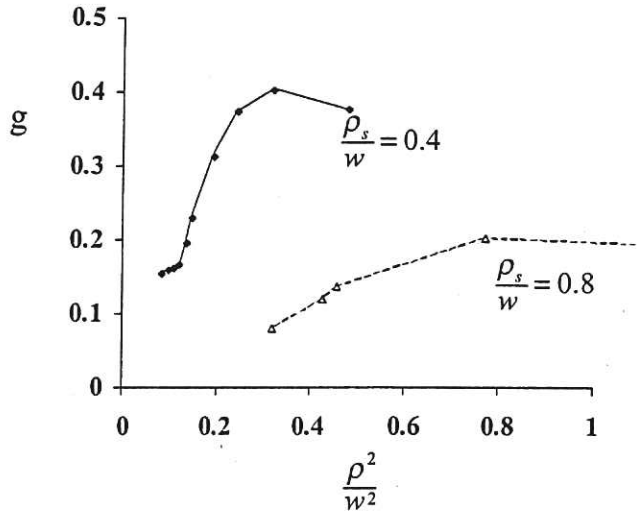

Figure 8: Plot of g versus $(\rho/w)^2 = (\rho_s/w)^2/(1 - \omega_{*e}/\omega)$ for the non-linear $K(\varphi)$ model with $\mu = D$. The curves show results for $\rho_s/w = 0.4$ (full curve) and $\rho_s/w = 0.8$ (dashed curve).

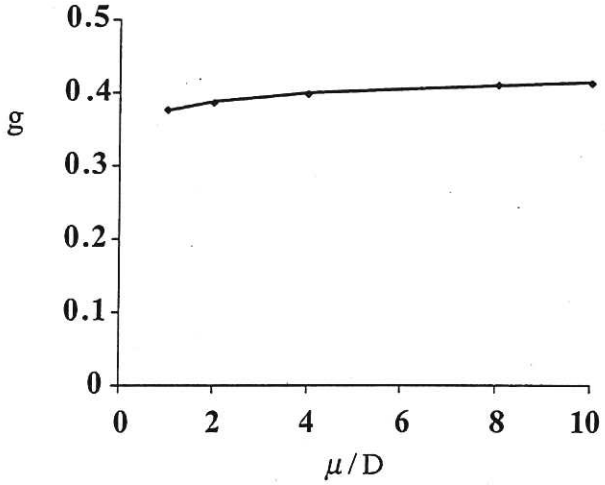

Figure 9: Variation of the coefficient g with the ratio of viscosity to radial diffusion, μ/D. Other parameters are fixed: $\omega/\omega_{*e} = 1.5$, $\rho_s/w = 0.4$.

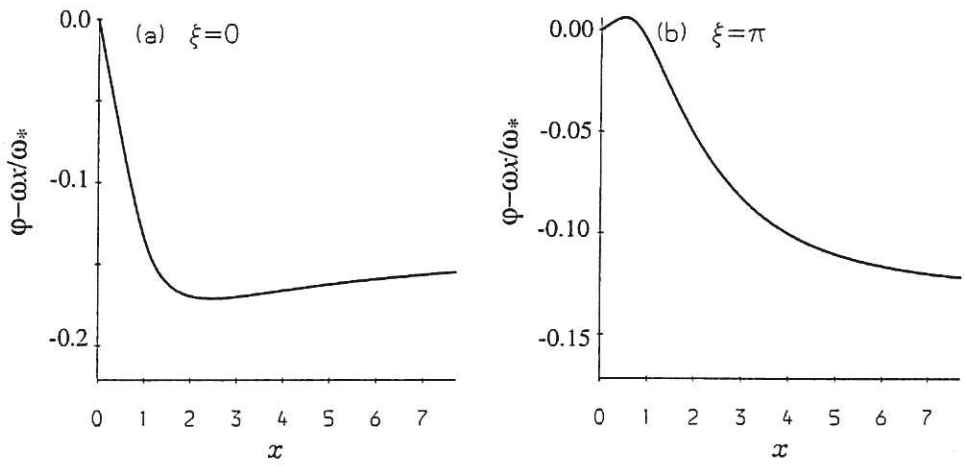

Figure 10: Variation of $\varphi - \omega x/\omega_{*e}$ with x for (a) $\xi = 0$ and (b) $\xi = \pi$ for $\mu/D = 10$; other parameters are as for Fig 9.

6 Conclusions

We have investigated the evolution of a small scale magnetic island in a sheared slab geometry, with particular attention to the processes taking place in the layer around the island separatrix. Our results show that the MHD model correctly predicts the destabilizing effect of the polarization current on island growth for mode rotation frequencies ω lying outside the drift-band $\omega_{*i} < \omega < \omega_{*e}$. The MHD model, however, substantially overestimates the magnitude of this effect.

The mode rotation frequency depends on the radial profiles of plasma flow, density and temperature. These radial profiles are determined by the conjunction of parallel and cross-field transport arising from viscosity, particle diffusion and thermal conduction. The transport is governed by a set of coupled, non-linear equations, (57) and (64), that determine the radial profiles in terms of the electrostatic potential φ. The electostatic potential itself is determined by an equation, Eq. (21), that is reminiscent of the Grad-Shafranov equation.

Surprisingly, we find that even in the presence of viscosity, the island rotates at a different velocity than the surrounding plasma as a result of diamagnetic effects. We estimate the width of the region where the plasma is entrained by the island to be $\sim \sqrt{\mu/D}\,\rho_s$. It is interesting to compare

our results to those of Monticello and White, [21] Biskamp [22], and Scott *et al.*[23]: Monticello and White found that diamagnetic mode rotation persists in the nonlinear regime, while Biskamp and Scott *et al.*, by contrast, found that it is nonlinearly arrested. The difference may be due to the effect of the sound wave, which was included by Biskamp [22] and Scott *et al.* [23], but omitted by Monticello and White [21] as well as in the present paper. The sound wave affects the rotation frequency by flattening the density profile and thus suppressing diamagnetic effects.[22, 23] Its role becomes significant for islands of width comparable to or greater than $\rho_s L_s / L_n$.

We have stated above that the polarization current is destabilizing for frequencies outside the drift-band $\omega_{*i} < \omega < \omega_{*e}$. We will show in a complementary paper, however, that it is *stabilizing* when the mode propagates in the ion drift band of frequency: that is, when the island is rotating in the ion diamagnetic drift direction but more slowly than the ion diamagnetic drift frequency, $\omega_{*i} < \omega < 0$. We will further show that the polarization current can be stabilizing in significant portions of the electron drift band, $0 < \omega < \omega_{*e}$. The result of the present work is thus to show the importance of the mode rotation frequency in the onset process for magnetic island growth, and to improve our knowledge of the conditions under which the polarization drift is stabilizing.

Although we believe that the work reported here represents a significant step forward in developing our understanding, we note the following two cautionary remarks:

1. Dissipation effects have been treated perturbatively. There is an additional sub-layer around the separatrix, assumed negligibly small here, where this is invalid and where perpendicular and parallel transport processes compete. In this sub-layer the density and temperature experience significant variation along flux surfaces [18].

2. In tokamaks, trapped particles provide a significant enhancement to the stabilizing contribution of the polarization current outside of the separatrix layer. It is unknown whether the destabilizing contribution of the layer is similarly enhanced.

Clearly, there is still much to be done to understand fully the role of the polarization current in tearing mode evolution.

Acknowledgment This work is funded in part by the United Kingdom

Department of Trade and Industry and Euratom, and by US DoE contract number DE-FG03-96ER-54346.

References

[1] X. Garbet, F. Mourgues and A. Samain, Plasma Phys. Controlled Fusion **30**, 343 (1988).

[2] X. Garbet, F. Mourgues and A. Samain, Plasma Phys. Controlled Fusion **32**, 131 (1990).

[3] P. H. Rebut and M. Hugon, Plasma Phys. Controlled Fusion **33**, 1085 (1990).

[4] A. I. Smolyakov, Sov. J. Plasma Phys. **15**, 667 (1989).

[5] A. I. Smolyakov, Plasma Phys. Controlled Fusion **35**, 657 (1993).

[6] M. Zabiego and X. Garbet, Phys. Plasmas **1**, 1890 (1994).

[7] J. W. Connor and H. R. Wilson, Phys. Plasmas **2**, 4575 (1995).

[8] A. I. Smolyakov, A. Hirose, E. Lazzaro, G. B. Re and J. D. Callen, Phys Plasmas **2**, 1581 (1995).

[9] H. R. Wilson, J. W. Connor, R. J. Hastie and C. C. Hegna, Phys Plasmas **3**, 248 (1996).

[10] H. R. Wilson, M. Alexander, J. W. Connor, A.M. Edwards et al, Plasma Phys. Controlled Fusion **38**, A149 (1996).

[11] F. L. Waelbroeck and R. Fitzpatrick, Phys. Rev. Lett. **78**, 1703 (1997).

[12] R. Fitzpatrick and F. L. Waelbroeck, Phys. Plasmas **7**, 1 (2000).

[13] A. B. Mikhailovskii, V. D. Pustovitov, A. I. Smolyakov and V. S. Tsypin, Phys. Plasmas **7**, 1214 (2000).

[14] S. I. Braginskii, Reviews of Plasma Physics Vol 1, ed M. Leontovich (New York: Consultants Bureau), 205 (1965).

[15] P. H. Rutherford, Phys. Fluids **16**, 1903 (1973).

[16] M. T. Kotschenreuther, R. D. Hazeltine, and P. J. Morrison, Phys. Fluids **28**, 294 (1985).

[17] D. Biskamp, Nucl. Fusion **18**, 1059 (1978).

[18] R. Fitzpatrick, Phys Plasmas **2**, 825 (1995).

[19] B. D. Scott and A. B. Hassam, Phys. Fluids **30**, 90 (1987).

[20] A. Sommerfeld, in '*Partial Differential Equations in Physics*' (Academic Press Inc., New York, 1949) Chapter III.

[21] D. A. Monticello and R. B. White, Phys. Fluids **23**, 366 (1980).

[22] D. Biskamp, Nucl. Fusion **19**, 777 (1979).

[23] B. D. Scott, A. B. Hassam, and J. F. Drake, Phys. Fluids **28**, 275 (1985).

99